Available online at www.sciencedirect.com
ScienceDirect
Journal of Molecular Catalysis A: Chemical 279 (2008) 133–139
JOURNAL OF MOLECULAR CATALYSIS A: CHEMICAL
www.elsevier.com/locate/molcata

A comparative study of strong metal–support interaction and catalytic behavior of Pd catalysts supported on micron- and nano-sized TiO_2 in liquid-phase selective hydrogenation of phenylacetylene

Patcharaporn Weerachawanasak [a], Piyasan Praserthdam [a], Masahiko Arai [b], Joongjai Panpranot [a,*]

[a] *Center of Excellence on Catalysis and Catalytic Reaction Engineering, Department of Chemical Engineering, Faculty of Engineering Chulalongkorn University, Bangkok, Thailand*
[b] *Division of Chemical Process Engineering, Graduate School of Engineering, Hokkaido University, Sapporo, Japan*

Received 21 September 2007; accepted 3 October 2007
Available online 9 October 2007

Abstract

The strong metal–support interaction and catalytic behaviors of Pd catalysts supported on micron(0.1 μm)- and nano-sized (14 nm) TiO_2 were investigated in the liquid-phase selective hydrogenation of phenylacetylene to styrene. It was found that when supported on the nano-sized TiO_2, the Pd/TiO_2 catalyst that reduced by H_2 at 500 °C exhibited strong metal–support interaction (SMSI) and much improved catalytic performance in liquid-phase selective hydrogenation of phenylacetylene. However, as revealed by CO pulse chemisorption, X-ray photoelectron spectroscopy (XPS), transmission electron microscopy (TEM), and CO-temperature program desorption, the SMSI effect was not detected for the micron-sized TiO_2 supported ones. It is suggested during high-temperature reduction, the inner Ti^{3+} in large crystallite size TiO_2 was more difficult to diffuse to the Pd^0 surface than the surface Ti^{3+} in the smaller crystallite size ones. Sintering of Pd^0 metal was observed instead.

Keywords: Pd/TiO_2; Liquid-phase hydrogenation; Phenylacetylene hydrogenation; Strong metal–support interaction

1. Introduction

The selective hydrogenation of alkynes to alkenes has fundamental importance in the fine chemicals production and industrial polymerization processes [1–4]. A large number of these reactions are carried out in liquid phase using batch type slurry reactors. The major advantages of supported noble metal catalysts in liquid-phase hydrogenation are their relatively high activity, mild process conditions, easy separation, and better handling properties. Pd is one of the most frequently used metals in such processes because of its unique ability to selectively hydrogenation.

Various supports have been employed for recent development of supported Pd catalysts for liquid-phase selective alkyne hydrogenation such as silica [5–8], MCM-41 [9–11], carbon [12], and titania [13–16]. Among these, titania is of particular interest because it exhibits the strong metal–support interaction (SMSI) phenomenon after reduction at high temperatures due to the decoration of the metal surface by partially reducible metal oxides [17,18] or by an electron transfer between the support and the metals [19,20]. In selective hydrogenation of acetylene to ethylene on Pd/TiO_2 catalysts, the charge transfer from Ti species to Pd weakened the adsorption strength of ethylene on the Pd surface hence higher ethylene selectivity was obtained [21]. Fan and coworkers [13] found that Pd/TiO_2 catalysts with SMSI exhibited higher selectivity for alkenes in liquid-phase hydrogenation of long chain alkadienes. Recently, Xu et al. [16] reported that Pd/TiO_2 catalyst prepared by sol–gel produced high conversion and high yield towards butyric acid in liquid-phase hydrogenation of maleic anhydride. The excellent catalyst performances were attributed to the strong interaction between metal and support and the formation of interfacial Pd–TiO_x site, which was induced by high-temperature reduction step.

Recently, there has been a growing interest in the application of nano-sized TiO_2 in the field of catalysis. With the

* Corresponding author. Tel.: +66 2218 6869; fax: +66 2218 6877.
E-mail address: joongjai.p@eng.chula.ac.th (J. Panpranot).

1381-1169/$ – see front matter © 2007 Elsevier B.V. All rights reserved.
doi:10.1016/j.molcata.2007.10.006

decrease in particle size to nanometer scale, photocatalytic activity of TiO_2 is enhanced because the optical band gap is widened due to surface defect [22,23] and an increase in surface area [24,25]. Various techniques have been reported for the preparation of nano-sized TiO_2 such as solvothermal method [26–28], precipitation method [29], sol–gel method [30–32], and thermal decomposition of alkoxide [33]. The sol–gel method is an easy method but the precipitated powders obtained are amorphous in nature and further heat treatment is required for crystallization. Solvothermal method is an alternative route for direct (one-step) synthesis of pure anatase TiO_2. Particle morphology, crystalline phase, and surface chemistry of the solvothermal-derived TiO_2 can be controlled by regulating precursor composition, reaction temperature, pressure, solvent property, and aging time.

In previous studies, the effect of TiO_2 polymorphs (anatase and rutile) on the strong metal–support interaction and catalytic properties of Pd/TiO_2 have been studied and compared [13,34]. It was shown that pre-reduction by H_2 at lower temperature results in SMSI for anatase titania supported palladium catalyst, but not for rutile titania supported one. A recent study from our group has shown that the use of pure anatase TiO_2 that contained significant amount of Ti^{3+} defects as supports for Pd catalysts gave high ethylene selectivities in gas-phase selective acetylene hydrogenation, while the use of pure rutile TiO_2 resulted in ethylene loss [35]. Nevertheless, the effects of Ti^{3+} and/or the TiO_2 crystallite size on the strong metal–support interaction of Pd/TiO_2 and their catalytic behavior in liquid-phase selective hydrogenation have never been reported.

Thus, it is the aim of this study to investigate the SMSI phenomena and catalytic behavior of Pd catalysts supported on micron- and nano-size TiO_2 in liquid-phase selective hydrogenation of phenylacetylene under mild reaction conditions. The nano-TiO_2 was synthesized by the solvothermal method in 1,4-butanediol using titanium *n*-butoxide as a titanium precursor. The catalysts were characterized by N_2 physisorption, X-ray diffraction (XRD), CO-temperature programmed desorption (CO-TPD), scanning electron microscopy (SEM), transmission electron microscopy (TEM), CO pulse chemisorption, electron spin resonance (ESR) and X-ray photoelectron spectroscopy (XPS).

2. Experimental

2.1. Preparation of TiO_2 and Pd/TiO_2 catalysts

The solvothermal-derived nano-TiO_2 was prepared according to the method described in Ref. [36] using 25 g of titanium(IV) *n*-butoxide (TNB) 97% from Aldrich. The starting material was suspended in 100 ml of 1,4-butanediol in a test tube and then set up in an autoclave. In the gap between the test tube and autoclave wall, 30 ml of solvent was added. After the autoclave was completely purged with nitrogen, the autoclave was heated to desired temperature (320 °C) at the rate of 2.5 K min^{-1} and held at that temperature for 6 h. Autogeneous pressure during the reaction gradually increased as the temperature was raised. After the reaction, the autoclave was cooled to room temperature. The resulting powders were collected after repeated washing with methanol by centrifugation. They were then air-dried at room temperature. For comparison purposes, the micron-sized anatase TiO_2 was obtained commercially from Aldrich. The micron- and nano-sized TiO_2 were denoted herein as TiO_2-micron and TiO_2-nano, respectively.

The 1%Pd/TiO_2 catalysts were prepared by the incipient wetness impregnation technique using an aqueous solution of the desired amount of $Pd(NO_3)_2{\cdot}6H_2O$ (Aldrich). The catalysts were dried overnight at 110 °C and then calcined in air at 450 °C for 3 h.

2.2. Catalyst characterization

The specific surface areas, pore volumes, and average pore diameters were determined by N_2 physisorption using a Micromeritics ASAP 2000 automated system and the Brunauer–Emmet–Teller (BET) method. Each sample was degassed under vacuum at $<1 \times 10^{-5}$ bar in the Micromeritics system at 150 °C for 4 h prior to N_2 physisorption. The XRD patterns of the catalysts were measured from 10° to 80° 2θ using a SIEMENS D5000 X-ray diffractometer and Cu Kα radiation with a Ni filter. The particle morphology was obtained using a JEOL JSM-35CF scanning electron microscope (SEM) operated at 20 kV. Catalyst crystallite sizes were obtained using the JEOL JEM 2010 transmission electron microscope that employed a LaB_6 electron gun in the voltage range of 80–200 kV with an optical point-to-point resolution of 0.23 nm. The amounts of CO chemisorbed on the catalysts were measured using a Micromeritic Chemisorb 2750 automated system with ChemiSoft TPx software. Prior to chemisorption, the sample was reduced in a H_2 flow at a desired temperature for 2 h and then cooled down to ambient temperature in a He flow. XPS analysis was performed using an AMICUS photoelectron spectrometer with Mg Kα X-ray as primary excitation and equipped with KRATOS VISION2 software. XPS elemental spectra were acquired with 0.1 eV energy step at pass energy of 75 kV. The C 1s line was taken as an internal standard at 285.0 eV. Electron spin resonance spectroscopy (ESR) was conducted using a JEOL JESRE2X electron spin resonance spectrometer. The intensity of ESR was calculated using a computer software program ES-PRIT ESR DATA SYSTEM version 1.6.

2.3. Reaction study

Approximately 0.2 g of 1%Pd/TiO_2 catalyst was placed into the 50 ml autoclave. The reactant consisting of 1 ml of phenyl acetylene and 9 ml of ethanol was mixed in a volumetric flask before being introduced into the autoclave reactor. Afterward the reactor is purged with hydrogen gas. The liquid-phase hydrogenation was carried out with H_2 pressure between 1 and 3 bar at 30 °C for 10–40 min. After the reaction, the vent valve was slowly opened to prevent the loss of product. The product mixture was analyzed by gas chromatography with flame ionization detector (FID).

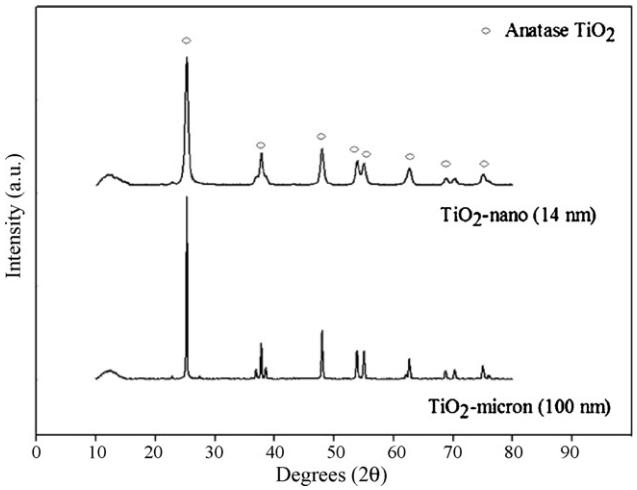

Fig. 1. XRD patterns of nano- and micron-sized TiO_2.

3. Results and discussion

Fig. 1 shows the XRD patterns of the micron- and nano-sized TiO_2. Both samples exhibited the characteristic peaks of the anatase titania at $2\theta = 25°$ (major), 37°, 48°, 55°, 56°, 62°, 71°, and 75°. The average crystallite sizes of the TiO_2-micron and TiO_2-nano calculated from the full width at half maximum of the XRD peak at $2\theta = 25°$ using the Scherrer equation were 100 nm (~0.1 μm) and 14 nm, respectively. The average crystallite size of TiO_2-micron in this study was found to be much larger than many commercially available TiO_2 widely used in the industry such as P-25 (Degussa), PC-500 and AT-1 (Millennium Chemicals), and Hombikat UV-100 (Sachtleben Chemie) in which the TiO_2 crystallite sizes are in the range of 10–30 nm [37]. The XRD characteristic peaks corresponding to PdO and/or Pd^0 metal were not observed after impregnation of Pd, calcination, and reduction steps due probably to the low amount of Pd present or a higher degree of Pd dispersion (results not shown).

Table 1 summarizes physicochemical properties of the TiO_2 and 1%Pd/TiO_2 catalysts. Reduction with H_2 either at 40 or 500 °C did not result in significant changes of the TiO_2 crystallite sizes. The BET surface area of the 1%Pd/TiO_2-micron was not altered from the original TiO_2-micron support suggesting that most of the palladium were deposited on the external surface of the support. In contrast, the BET surface areas of the TiO_2-nano decreased after Pd loading followed by the high-temperature reduction at 500 °C, indicating that Pd was deposited in some of the pores of the TiO_2 support. A slight increase in the TiO_2 crystallite sizes of the TiO_2-nano from 14 to 17 nm was probably caused by high temperature calcination and reduction of the catalysts at 500 °C. The percentage of Pd dispersion estimated from CO chemisorption and Pd^0 metal particle sizes calculated were also given in Table 1. It was found that %Pd dispersion decreased when the catalysts were reduced at 500 °C for both TiO_2-micron and TiO_2-nano-supported Pd catalysts. However, %Pd dispersion for 1%Pd/TiO_2-micron decreased by 80.5% while that of 1%Pd/TiO_2-nano decreased by only 53.5%. The corresponding Pd^0 particle sizes calculated based on CO chemisorption were varied from 6.7 to 48.7 nm.

Fig. 2 shows the SEM micrographs of TiO_2 and 1%Pd/TiO_2 catalysts (calcined). The TiO_2-micron had a uniform particle size of 0.1–0.2 μm while the TiO_2-nano consisted of irregular shape of very fine agglomerated particles. Morphologies of the reduced 1%Pd/TiO_2 catalysts were not significantly different from the corresponding TiO_2 supports suggesting high-thermal stability of the TiO_2. TEM analysis has been carried out in order to physically measure the Pd^0 particle sizes on the various TiO_2 supports and the results are shown in Fig. 3. The particle sizes of various TiO_2 supports were consistent to those obtained from XRD results. It is clearly seen that on the TiO_2-micron, Pd^0 metal particle sizes increased when the catalyst was reduced at 500 °C whereas those on the TiO_2-nano were essentially the same to those reduced at 40 °C. Such results indicate that sintering of Pd^0 metal occurred on the 1%Pd/TiO_2-micron catalyst during high-temperature reduction, in agreement with the lower amount of CO chemisorption observed (Table 1). For the 1%Pd/TiO_2-nano reduced at 500 °C, the results of TEM and low CO chemisorption (giving an over estimation of the Pd^0 metal particle sizes) indicate that the catalyst exhibited strong metal–support interaction under high-temperature reduction since no change in the Pd^0 particle size was observed. The SMSI effect on these catalysts was confirmed by measuring the amounts of CO chemisorption of the re-calcined (at 450 °C) and re-reduced (at 40 °C) catalysts after they were subjected to reduction at 500 °C. The results are illustrated in Fig. 4. The amount of CO chemisorption of the re-calcined and re-reduced 1%Pd/TiO_2-micron was less than that reduced at 40 °C suggesting that sintering of Pd^0 occurred during high-

Table 1
Physicochemical properties of various TiO_2 and 1%Pd/TiO_2 catalysts

Sample[a]	Crystallite size of TiO_2 by XRD (nm)	BET (m^2/g)	Pore volume (cm^3/g)	Pore diameter (nm)	%Pd dispersion[b]	d_pPd^0 (nm)[c]
TiO_2-micron	100	10	0.02	7.6	–	–
TiO_2-nano	14	79	0.40	14.9	–	–
1%Pd/TiO_2-micron-R40	96	9	0.03	1.3	16.4	6.9
1%Pd/TiO_2-micron-R500	94	11	0.03	1.2	3.2	48.7
1%Pd/TiO_2-nano-R40	16	73	0.31	0.6	16.8	6.7
1%Pd/TiO_2-nano-R500	17	68	0.28	0.8	7.8	40.6

[a] R40 and R400 indicate the samples reduced at 40 and 500 °C, respectively.
[b] Determined from CO chemisorption.
[c] Based on d (nm) = (1.12/D) [46], where D is the fractional metal dispersion.

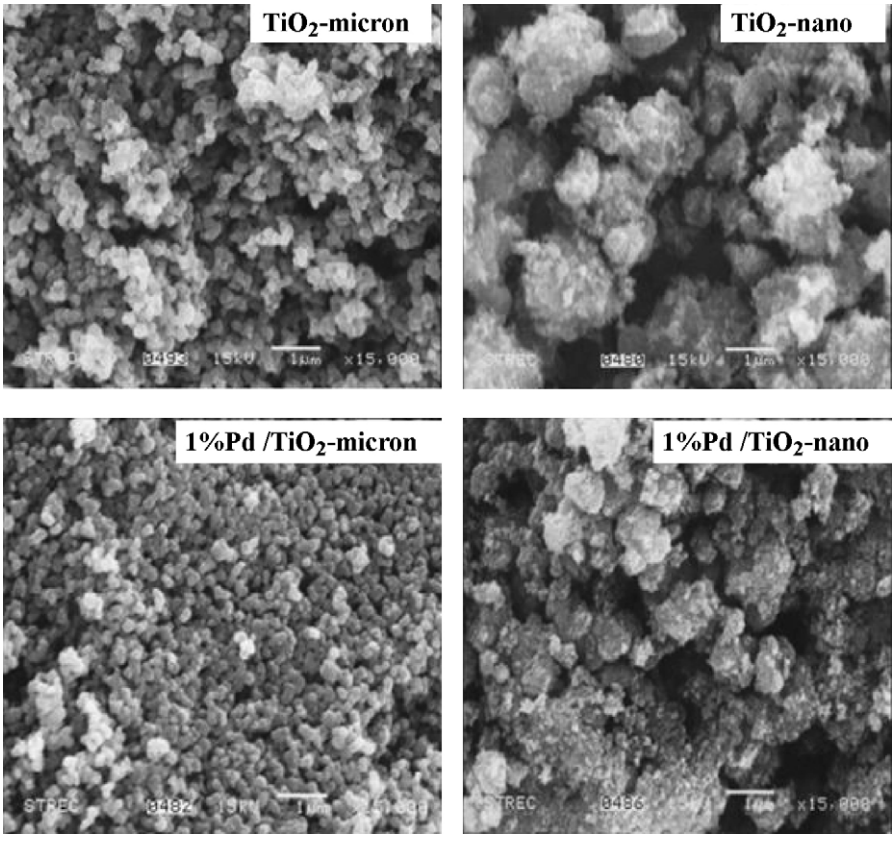

Fig. 2. SEM micrographs of TiO_2 and 1%Pd/TiO_2 (calcined).

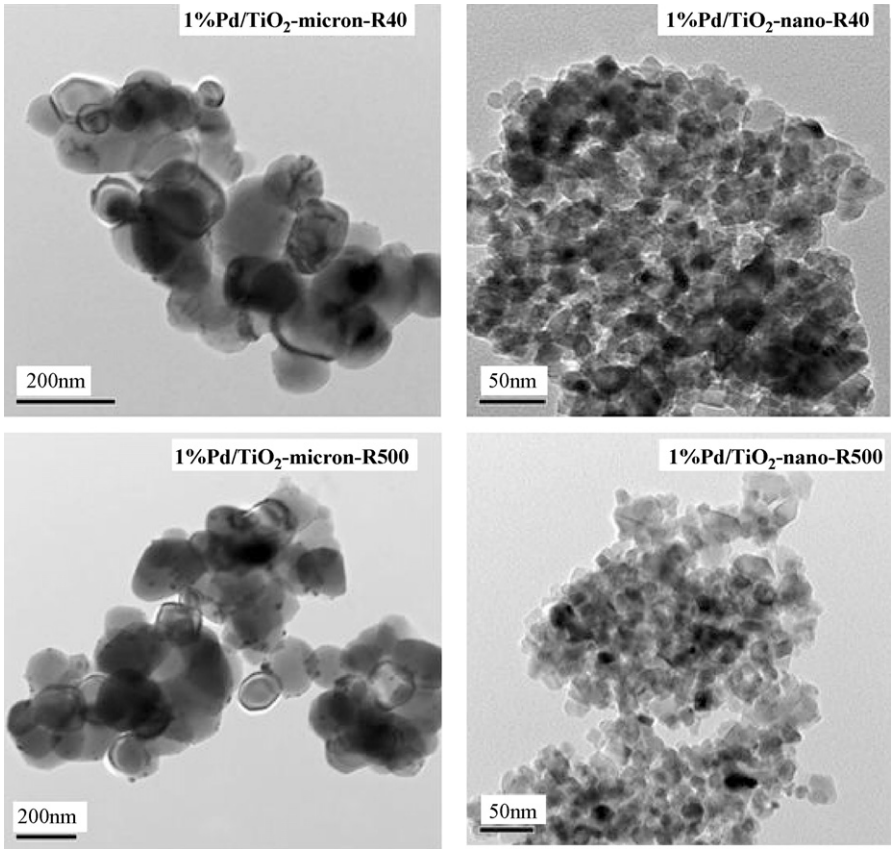

Fig. 3. TEM micrographs of the various Pd/TiO_2 catalysts.

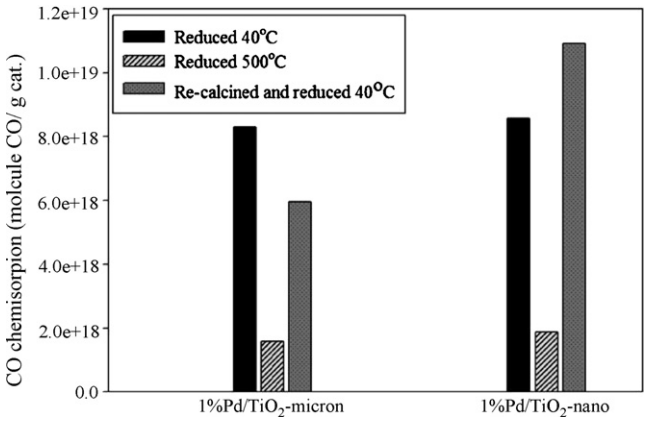

Fig. 4. CO chemisorption results.

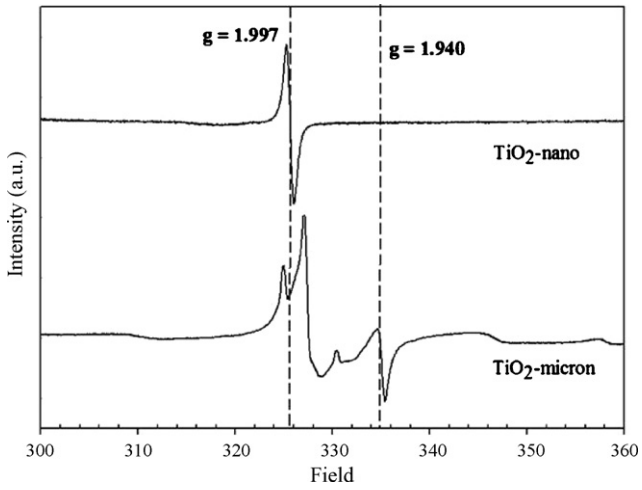

Fig. 5. ESR spectra of nano- and micron-sized TiO_2.

temperature reduction while the amount of CO chemisorption of the re-calcined and re-reduced 1%Pd/TiO_2-nano can be totally recovered. It is generally known that strong metal–support interaction in TiO_2 supported Pd catalysts occurred after a high-temperature reduction ≥500 °C. It is thus surprising that such interaction was not detected on our 1%Pd/TiO_2-micron. However, it should be noticed that the TiO_2 crystallite sizes used for preparation of Pd/TiO_2 catalysts in most studies in the literature were in nanometer range (usually less than 50 nm) [13–15,38]. Panagiotopoulou et al. [39] also reported that formation of sub-stoichiometric TiO_x species started at lower temperature and was more facile over Pt/TiO_2 for small TiO_2 particle sizes (10–35 nm). On the other hand, a recent study by Musolino et al. [14] on the selective liquid-phase hydrogenation of *cis*-2-butene-1,4-diol to 2-hydroxy tetrahydrofuran on various supported Pd catalysts revealed the absence of SMSI effect for the Pd/TiO_2 catalyst reduced at high temperature. The interpretation of the observed behavior has not been given by those authors. However, the TiO_2 support used in their study was also anatase-phase TiO_2 from Aldrich with the specific surface area of ∼9 m^2/g similar to the micron-sized TiO_2 reported in this study.

The surface compositions of the catalysts as well as the interaction between Pd and the TiO_2 supports were confirmed by XPS analysis. The binding energies, FWHM, and atomic concentrations of Ti 2p, O 1s, and Pd 3d on various Pd/TiO_2 catalysts are given in Table 2. The Ti/O atomic ratios were found to be much higher for the TiO_2-nano than the TiO_2-micron suggesting that the solvothermal-derived TiO_2-nano possessed more oxygen vacancies (or so-called Ti^{3+} defective sites) on the TiO_2 surface than the TiO_2-micron. However, there was also probably an oxygen-rich layer near the surface of the TiO_2 particles, which was formed by oxygen adsorption and easy oxidation of titanium surface [40]. When reduced at 500 °C, the Pd/Ti surface concentration decreased by 15 and 55% for 1%Pd/TiO_2-micron and 1%Pd/TiO_2-nano, respectively. A slight decrease of Pd/Ti surface concentration for 1%Pd/TiO_2-micron may be due to larger Pd^0 particle size formed by sintering as shown by TEM and CO chemisorption, while a large decrease of Pd/Ti on the 1%Pd/TiO_2-nano would be due to decoration of Pd^0 metal surface by the reducible TiO_2 support. The binding energies of Pd $3d_{5/2}$ (335.0–335.2 eV) and the FWHM less than 2 eV revealed that palladium was in the form of Pd^0 metal for both cases [41].

The presence of Ti^{3+} in both TiO_2-micron and TiO_2-nano supports was revealed by electron spin resonance technique (Fig. 5). The Ti^{3+} species are produced by trapping of electrons at defective sites of TiO_2 and the amount of accumulated electrons may therefore reflect the number of defective sites [42]. The signal of *g* value less than two was assigned to Ti^{3+} ($3d^1$) [43]. Nakaoka et al. [44] reported six signals of ESR measurement occurring on the surface of titania: (i) $Ti^{4+}O^-Ti^{4+}OH^-$, (ii) surface Ti^{3+}, (iii) adsorbed oxygen (O^{2-}), (iv) $Ti^{4+}O^{2-}Ti^{4+}O^{2-}$, (v) inner Ti^{3+}, and (vi) adsorbed water. In this study, it is clearly seen that the solvothermal-derived TiO_2 exhibited only one strong ESR signal at a *g* value of 1.997, which can be attributed

Table 2
XPS results

Catalysts	Ti 2p		O 1s		Pd 3d		Atomic concentration	
	B.E. (eV)	FWHM	B.E. (eV)	FWHM	B.E. (eV)	FWHM	Ti/O	Pd/Ti
TiO_2-micron	458.6	1.259	532.3	2.362	–	–	0.028	–
TiO_2-nano	458.7	1.308	530.0	1.675	–	–	0.204	–
1%Pd/TiO_2-micron R40	458.7	1.516	530.2	2.324	335.0	1.704	0.123	0.073
1%Pd/TiO_2-micron R500	458.7	1.846	530.2	1.846	335.2	1.849	0.178	0.062
1%Pd/TiO_2-nano-R40	458.7	1.292	530.0	1.596	335.0	1.570	0.210	0.009
1%Pd/TiO_2-nano-R500	458.6	1.319	529.9	1.681	*n/d*	*n/d*	0.190	0.004

to Ti^{3+} at the surface. Many Ti^{3+} ESR signals were observed for the TiO_2-micron indicating that more than one type of Ti^{3+} defects were presented in the sample, i.e., surface Ti^{3+} and inner Ti^{3+}. Moreover, less amount of surface Ti^{3+} was present on the micron-sized TiO_2. Literature data indicate that the presence of Ti^{3+} promotes strong metal–support interaction in Pd/TiO_2 catalysts since Ti^{3+} can easily diffuse from the lattice of TiO_2 to surface of Pd particles [13]. The results in this study, however, have shown that probably only the surface Ti^{3+} has high mobility and the other Ti^{3+} species may not be able to diffuse easily to Pd^0 surface so that Pd catalyst supported on the TiO_2-micron with significant amount of Ti^{3+} did not exhibited the strong metal–support interaction.

Temperature programmed desorption of CO has been carried out in order to elucidate the influence of TiO_2 crystallite size, Pd dispersion, and reduction temperature on the strength and mechanism of CO adsorption on TiO_2 supported Pd catalysts. The results are shown in Fig. 6. For $1\%Pd/TiO_2$-micron reduced at 40 °C, two main desorption peaks were observed at ca. 340 and 640 °C which may be attributed to CO adsorbed on different adsorption sites probably Pd^0 with different particle sizes and/or adsorption on Ti^{3+} sites [45]. Both peaks were slightly

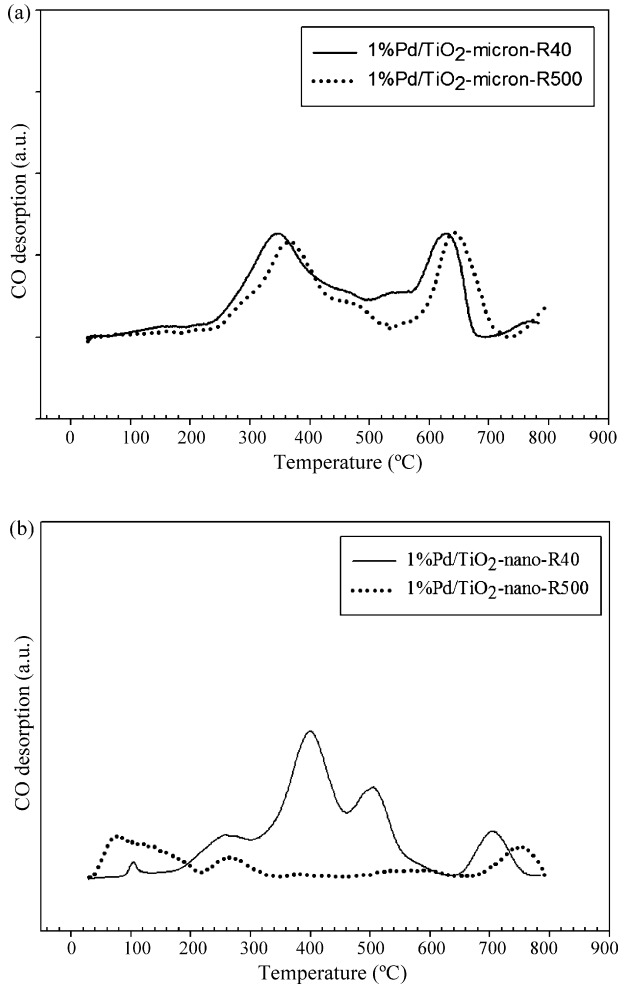

Fig. 6. CO-temperature programmed desorption profiles of (a) micron- and (b) nano-sized TiO_2 supported Pd catalysts.

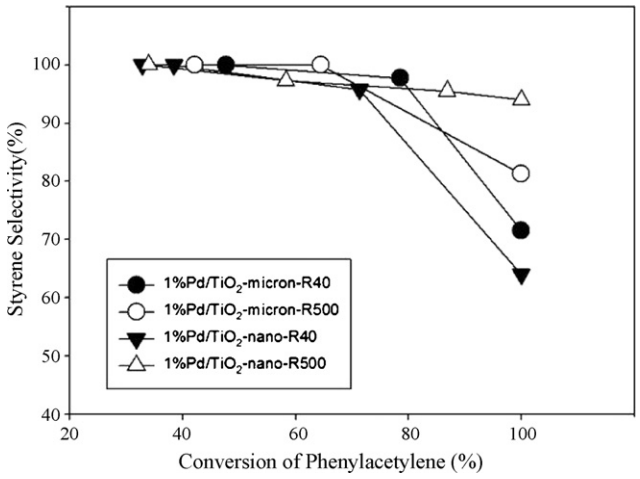

Fig. 7. Catalyst performances in liquid-phase selective hydrogenation of phenylacetylene.

shifted to higher temperature for the catalyst reduced at 500 °C. However, the amounts of CO desorption were not significant different for $1\%Pd/TiO_2$-micron reduced at 40 or 500 °C indicating that CO adsorption strength was not much different for the catalysts reduced at low and high temperatures. In contrast, $1\%Pd/TiO_2$-nano reduced at 40 °C exhibited several desorption peaks at 100–800 °C indicating various adsorption sites on the catalyst surface. However, the peaks become almost flat when the catalyst was reduced at 500 °C indicating negligible CO adsorption under such conditions. In other words, CO was weakly adsorbed under high-temperature reduction conditions due to the strong metal–support interaction effect.

Fig. 7 shows the performance of the $1\%Pd/TiO_2$-micron and $1\%Pd/TiO_2$-nano catalysts in liquid-phase selective hydrogenation of phenylacetylene under mild conditions. Both catalysts exhibited high styrene selectivities (≥95%) for phenylacetylene conversions less than 80%. Based on the conditions and the column used in our GC analysis, the other product found in the reaction besides styrene was ethylbenzene. No other by-products were observed. The selectivity for styrene significantly dropped to 65–80% when conversion of phenylacetylene reached 100% for all the catalysts except $1\%Pd/TiO_2$-nano reduced at 500 °C that retained its high styrene selectivity >90%. Such results suggest that the strong metal–support interaction on $1\%Pd/TiO_2$-nano catalyst produced great beneficial effect on the catalyst performance. The presence of SMSI effect may result in an inhibition of the adsorption of the product styrene on the $1\%Pd/TiO_2$-nano; hence high styrene selectivity was obtained.

The turnover frequencies (TOF) values were calculated from the data at a small conversion level of, for example, 30% for the catalysts except for the SMSI catalyst. It was found that the TOFs increased from 5.5 s^{-1} for $1\%Pd/TiO_2$-micron-R40) to 25.1 s^{-1} for $1\%Pd/TiO_2$-micron-R500) corresponding to the increase of Pd^0 particle size from 7 to 49 nm, respectively. The amount of exposed Pd species were estimated from CO chemisorption data with the assumption that one carbon monoxide molecule adsorbs on one palladium site [46–51]. The specific activity results were found to be in agreement with the well-established trend in the

literature that the liquid-phase hydrogenation activity decreases as Pd^0 particle size decreases [52–58].

4. Conclusions

As revealed by various analytical techniques such as CO pulse chemisorption, X-ray photoelectron spectroscopy (XPS), transmission electron microscopy (TEM), and CO-temperature program desorption, reduction by H_2 at 500 °C resulted in strong metal–support interaction for the nano-sized TiO_2 supported Pd catalyst, but not for the micron-sized TiO_2 supported one. The SMSI effect, however, appeared to be necessary for high catalytic performance of the Pd/TiO_2 catalysts in the liquid-phase selective hydrogenation of phenylacetylene to styrene.

Acknowledgements

Financial supports from the Thailand Research Fund (TRF), the Graduate School of Chulalongkorn University (the 90th Anniversary of Chulalongkorn University-the Golden Jubilee Fund), and the Commission on Higher Education, Thailand are gratefully acknowledged.

References

[1] L. Guczi, A. Horvath, A. Beck, A. Sarkany, Stud. Surf. Sci. Catal. 145 (2003) 351.
[2] O. Dominguez-Quintero, S. Martinez, Y. Henriquez, L. D'Ornelas, H. Krentzien, J. Osuna, J. Mol. Catal. A 197 (2003) 185.
[3] K.J. Stanger, Y. Tang, J. Anderegg, R.J. Angelici, J. Mol. Catal. A 202 (2003) 147.
[4] T.A. Nijhuis, G. van Koten, J.A. Moulijn, Appl. Catal. A 238 (2003) 259.
[5] J.W. Park, Y.M. Chung, Y.W. Suh, H.K. Rhee, Catal. Today 93 (2004) 445.
[6] N. Marin-Astorga, G. Pecchi, J.L.G. Fierro, P. Reyes, Catal. Lett. 91 (2003) 115.
[7] N. Marin-Astorga, G. Pecchi, T.J. Pinnavaia, G. Alvez-Manoli, P. Reyes, J. Mol. Catal. A 247 (2006) 145.
[8] J. Panpranot, K. Phandinthong, T. Sirikajorn, M. Arai, P. Praserthdam, J. Mol. Catal. A 261 (2007) 29.
[9] A. Papp, A. Molnar, A. Mastalir, Appl. Catal. A 289 (2005) 256.
[10] A. Mastalir, B. Rac, Z. Kiraly, A. Molnar, J. Mol. Catal. A 264 (2007) 170.
[11] S. Sato, R. Takahashi, T. Sodesawa, M. Koubata, Appl. Catal. A 284 (2005) 247.
[12] D. Teschner, E. Vass, M. Hävecker, S. Zafeiratos, P. Schnörch, H. Sauer, A. Knop-Gericke, R. Schlögh, M. Chamam, A. Wootsch, A.S. Canning, J.J. Gamman, S.D. Jackson, J. MacGregor, L.F. Gladden, J. Catal. 242 (2006) 26.
[13] Y. Li, B. Xu, Y. Fan, N. Feng, A. Qiu, J. Miao, J. He, H. Yang, Y. Chen, J. Mol. Catal. A 216 (2004) 107.
[14] M.G. Musolino, P. De Maio, A. Donato, R. Pietropaolo, J. Mol. Catal. A 208 (2004) 219.
[15] M.G. Musolino, G. Apa, A. Donato, R. Pietropaolo, F. Frusten, Appl. Catal A 25 (3) (2007) 112.
[16] J. Xu, K. Sun, L. Zhang, Y. Ren, X. Xu, Catal. Commun. 6 (2005) 462.
[17] J. Santos, J. Phillips, J.A. Dumesic, J. Catal. 81 (1983) 147.
[18] G.B. Raupp, J.A. Dumesic, J. Catal. 95 (1985) 587.
[19] J.M. Herrmann, M. Gravelle-Rumeau-Maillot, P.C. Gravelle, J. Catal. 104 (1987) 136.
[20] P. Chou, M.A. Vannice, J. Catal. 104 (1987) 1.
[21] J.H. Kang, E.W. Shin, W.J. Kim, J.D. Park, S.H. Moon, J. Catal. 208 (2002) 310.
[22] C. Shifu, C. Gengyu, Surf. Coat. Technol. 200 (2006) 3637.
[23] K. Suriye, P. Praserthdam, B. Jongsomjit, Ind. Eng. Chem. Res. 44 (2005) 6599.
[24] R.K. Madhusudan, C.V. Gopal, S.V. Manorama, J. Solid State Chem. 158 (2001) 180.
[25] T. Toyoda, H. Kawano, Q. Shen, A. Kotera, M. Ohmori, Jpn. J. Appl. Phys. 39 (2000) 3160.
[26] C.-S. Kim, B.K. Moon, J.-H. Park, S.T. Chung, S.-M. Son, J. Cryst. Growth 254 (2003) 405.
[27] C. Wang, Z.-X. Deng, G. Zhang, S. Fan, Y. Li, Powder Technol. 125 (2002) 39.
[28] M. Kang, B.-J. Kim, S.M. Cho, C.-H. Chung, B.-W. Kim, G.Y. Han, K.J. Yoon, J. Mol. Catal. A 180 (2002) 125.
[29] H.-D. Nam, B.-H. Lee, S.-J. Kim, C.-H. Jung, J.-H. Lee, S. Park, Jpn. J. Appl. Phys. 37 (1998) 4603.
[30] C. Su, B.-Y. Hong, C.-M. Tseng, Catal. Today 96 (2004) 119.
[31] Y. Bessekhouad, D. Robert, J.V. Weber, J. Photochem. Photobiol. A: Chem. 157 (2003) 47.
[32] M.J. Alam, D.C. Cameron, J. Sol–Gel Sci. Technol. 25 (2002) 137.
[33] H. Kominami, J.-I. Kalo, Y. Takada, Y. Doushi, B. Ohtani, S.-I. Nishimoto, M. Inoue, Y. Kera, Catal. Lett. 46 (1997) 235.
[34] J. Panpranot, K. Kontapakdee, P. Praserthdam, J. Phys. Chem. B 110 (2006) 8019.
[35] J. Panpranot, K. Kontapakdee, P. Praserthdam, Appl. Catal. A 314 (2006) 128.
[36] W. Payakgul, O. Mekasuwandumrong, V. Pavarajarn, P. Praserthdam, Ceram. Int. 31 (2005) 391.
[37] P. Panaglotopoulou, D.I. Kondarides, J. Catal. 225 (2004) 327.
[38] R.F. Hicks, A.T. Bell, J. Catal. 90 (1984) 205.
[39] P. Panagiotopoulou, A. Christodoulakis, D.I. Kondarides, S. Boghosian, J. Catal. 40 (2) (2006) 114.
[40] F. Zhang, Z. Zheng, D. Liu, Y. Mao, Y. Chen, Z. Zhou, S. Yang, X.X. Liu, Phys. Res. B 132 (1997) 620.
[41] C.D. Wagner, W.M. Riggs, L.E. Davis, J.F. Moulder, in: G.E. Muilenberg (Ed.), Handbook of X-ray Photoelectron Spectroscopy, Perkin-Elmer Corporation, Eden Prairie, MN, 1978.
[42] S. Ikeda, N. Sugiyama, S. Murakami, H. Kominami, Y. Kera, H. Noguchi, K. Uosaki, T. Torimoto, B. Ohtani, Phys. Chem. Chem. Phys. 5 (2003) 778.
[43] T.M. Salama, H. Hattori, H. Kita, K. Ebitani, T. Tanaka, J. Chem. Soc., Faraday Trans. 89 (1993) 2067.
[44] Y. Nakaoka, Y. Nosaka, J. Photochem. Photobiol. A 110 (1997) 299.
[45] E.V. Benvenutti, L. Franke, C.C. Moro, Langmuir 15 (1999) 3140.
[46] N. Mahata, V. Vishwanathan, J. Catal. 196 (2000) 262.
[47] S.H. Ali, J.G. Goodwin Jr., J. Catal. 176 (1998) 3.
[48] E.A. Sales, G. Bugli, A. Ensuque, M.J. Mendes, F. Bozon-Verduraz, Phys. Chem. Chem. Phys. 1 (1999) 491.
[49] A. Sarkany, Z. Zsoldos, B. Furlong, J.W. Hightower, L. Guczi, J. Catal. 41 (1993) 566.
[50] M.A. Vannice, S.Y. Wang, S.H. Moon, J. Catal. 71 (1981) 152.
[51] N.K. Nag, Catal. Lett. 24 (1994) 37.
[52] N. Marin-Astroga, G. Alvez-Manoli, P. Reyes, J. Mol. Catal. A 226 (2005) 81.
[53] A. Molnar, A. Sarkany, M. Varga, J. Mol. Catal. A 173 (2001) 185.
[54] D. Duca, L.F. Liotta, G. Deganello, J. Catal. 154 (1995) 69.
[55] G. Carturan, G. Facchin, G. Cocco, S. Enzo, G. Navazio, J. Catal. 76 (1982) 405.
[56] A. Sarkany, A.H. Weiss, L. Guczi, J. Catal. 98 (1986) 550.
[57] P. Albers, K. Seibold, G. Prescher, H. Muller, Appl. Catal. A 146 (1999) 135.
[58] G. del Angel, J.L. Benitez, J. Mol. Catal. A 94 (1994) 409.